

Seismic Performance of Reinforced Concrete Beams with Low Strength Concrete

TANIGUCHI HIROAKI¹, YASOJIMA AKIRA², ARAKI HIDEO³

¹ Graduate Student, Dept. of Social and Environmental Engineering, Hiroshima University, Hiroshima, Japan

² Assistant Prof., Dept. of S.E. Eng., Hiroshima Univ., Japan

³ Assoc. Prof., Dept. of S.E. Eng., Hiroshima Univ., Japan

Email: taniguchi-hiroaki@hiroshima-u.ac.jp

ABSTRACT :

Two series of experimental works concerning low strength concrete of the existing reinforced concrete buildings was performed, in order to provide the appropriate seismic evaluation method for low strength concrete buildings in this study. Material tests of low strength concrete were performed to obtain the fundamental characteristics of low strength concrete. Then, the monotonic loading tests of beams whose parameters were concrete strength and stirrup ratio were performed to investigate the shear capacity of the structural member used low strength concrete. From test results it was founded that modified Popovics model for stress strain curves of concrete was applicable for low strength concrete, and shear capacity could be estimated by the present formula based on arch and truss theory.

KEYWORDS: Low strength concrete, Stress strain curve, Popovics model, Shear capacity

1. INTRODUCTION

1.1. The Presence of Low Strength Concrete

Seismic evaluations for existing RC buildings had been made extensively in Japan after Hyogoken-Nanbu earthquake in 1995. According to the some reports, the very low strength of the concrete cores from the existing RC buildings which were less than half of design concrete strength were frequently found in seismic evaluations. It was reported that many number of low strength concrete less than 10MPa were found in concretes cores from buildings constructed at 1960s to 1970s, though design strength of 180kgf/cm² (18MPa) before the building standards revision in 1970 were usually used in Japan in the previous studies^{[1],[2]} Concrete cores of which strength were less than 13.5MPa reached 6.1% of total inspected cores.

1.2. The Present Conditions of the Seismic Evaluation

The recommended lower limit of concrete strength is 13.5MPa in Standard for Seismic Evaluation of Existing Reinforced Concrete Building^[3]. However, even when concrete strength is lower than that limit strength, the seismic evaluation method is performed to those existing buildings, though it is unconfirmed that the formulas in the standard can be applicable for the existing RC building of low strength concrete less than 13.5MPa.

1.3. Purpose of this Study

To investigate the performance of the low strength concrete buildings it is necessary know how to manufacture the low strength concrete less than 13.5MPa as first step of this study. So, material test considering water cement ratio as a main parameter was performed to obtain how to manufacture low strength concrete. Based on the material tests, the monotonic loading tests under the anti-symmetric moment with one-third scaled RC beams were carried out to obtain the shear and bond characteristics of structural members used low strength concrete.

2. MATERIAL PROPERTIES

Four patterns of water cement ratio 70, 93, 110, and 140% were considered in the material test to manufacture the low strength concrete less than 13.5MPa. After curing for 7 days, 28 days and 91 days, the compressive and splitting tests with concrete cylinders were performed to obtain the fundamental mechanical properties of the low strength concrete.

2.1 Mix properties

Mix properties of concrete are shown in Table 2.1. Mix properties of LS70 and LS110 were based on Recommendation for Practice of Mix Design of Concrete^[4] of Architectural Institute of Japan (AIJ). Amount of cement in LS93 and LS140 were reduced by approximately 75% and 50% cement of LS70, respectively. Design compressive strength estimated by Eq. 2.1 in Japanese Architectural Standard Specification for Reinforced Concrete Work (JASS 5)^[5] of AIJ is also shown in Table 2.1.

Table 2.1 Summaries of mix properties for concrete

Mix type	Design strength (MPa)	Water cement Ratio (%)	Cement (kg/m ³)	Water (kg/m ³)	Sand (kg/m ³)	Aggregate (kg/m ³)	Slump (mm)	Sand percentage (%)	Air content (%)
LS70	25.1	70	271	189.7	933	859	185	52	4.8
LS93	14.3	93	203	189.7	933	859	185	52	4.8
LS110	9.2	110	209	229.9	905	834	180	52	4.8
LS140	3.3	140	135.5	189.7	933	859	185	52	4.8

$$x = \frac{51}{F/K + 0.31} \quad (\%) \quad (2.1)$$

where

x : Water cement ratio
 F : Design strength (MPa)
 K : Strength of cement (=60) (MPa)

2.2. Results of Material Test

2.2.1. Compressive strength

Compressive strengths are shown in the left columns of Table 2.2. Fig. 2.1 shows relationship between compressive strength and water cement ratio. The broken line calculated by JASS 5 was also inserted in Fig. 2.1. Observed strength of 28 days agreed with the calculated ones except for LS140. From the results of the material test the mixture of LS110 (water cement ratio 110%) was used for concrete of the next beam tests.

2.2.2. Young's modulus

Young's modulus are shown in the middle columns of Table 2.2. Fig. 2.2 shows relationship between Young's modulus and compressive strength. The broken line in Fig. 2.2 is calculated value by Eq. 2.2 which is shown in Standard for Structural Calculation of Reinforced Concrete Structures -Based on Allowable Stress Concept^[6] of AIJ. This line of the standard corresponds approximately to test results.

$$E_c = 33.5 \times \left(\frac{\gamma}{24}\right)^2 \times \left(\frac{\sigma_B}{60}\right)^{\frac{1}{3}} \quad (\text{GPa}) \quad (2.2)$$

where

E_c : Young's modulus
 γ : Density of the concrete
 σ_B : Concrete compressive strength (MPa)

2.2.3. Strain at the maximum stress

The strains at the maximum stress are shown in right columns of Table 2.2. From the test results, when water cement ratio increased, stress at the maximum stress increased. In other words, when compressive strength decreased, the strain at the maximum stress became large. Fig. 2.3 shows representative relationship between stress and strain of each mixing type.

Table 2.2 Mechanical properties of concrete

Mix type	Water cement ratio (%)	Compressive strength (MPa)			Young's modulus (GPa)			Strain at the maximum stress (%)		
		7days	28days	91days	7days	28days	91days	7days	28days	91days
LS70	70	17.6	23.3	24.9	23.6	19.5	26.9	0.219	0.241	0.233
LS93	93	10.9	13.5	15.1	21.0	22.6	24.9	0.261	0.209	0.239
LS110	110	7.6	9.9	11.3	21.8	19.8	18.1	0.381	0.409	0.381
LS140	140	5.2	5.9	7.0	9.9	9.3	13.1	0.412	0.703	0.401

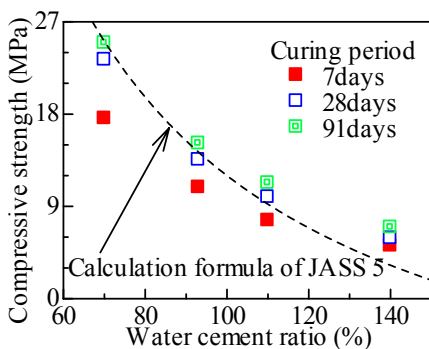


Fig. 2.1 Compressive strength vs. water cement ratio

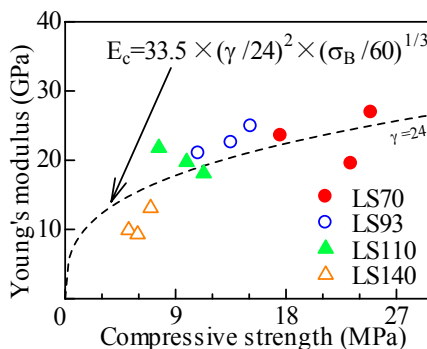


Fig. 2.2 Young's modulus vs. compressive strength

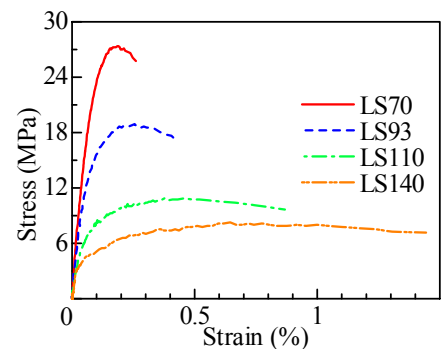


Fig. 2.3 Stress and strain curves

2.3. Modeling for Relationship between Stress and Strain

The comparisons between Popovics model and observed results of stress strain curves are shown in Fig. 2.4. Popovics model can not describe initial stiffness on low strength.

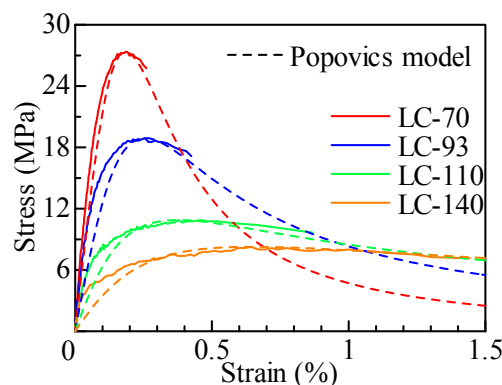


Fig. 2.4 Comparisons between Popovics model and observed stress strain curves

Popovics proposed that stress strain curve for normal strength concrete was expressed by Eq. 2.3 using the observed maximum compressive stress σ_B , the experimental constant n and ξ ($\varepsilon/\varepsilon_m$). The experimental constant is expressed by Eq. 2.4. The strain at the maximum stress is expressed by Eq. 2.6. Because Popovics model depends on experimental constant, it is necessary for low strength concrete to modify the experimental constant n .

$$\sigma = \sigma_B \frac{n \cdot \xi}{n - 1 + \xi^n} \quad (2.3)$$

$$n = 0.0582\sigma_B + 1 \quad (2.4)$$

$$\xi = \frac{\varepsilon}{\varepsilon_m} \quad (2.5)$$

$$\varepsilon_m = 7674\sqrt{\sigma_B} \quad (\mu) \quad (2.6)$$

where

σ : Compressive stress (MPa)

σ_B : Observed maximum compressive stress

n : Experimental constant

ε : Strain

ε_m : Strain at maximum stress

Murakami modified experimental constant n and strain at the maximum stress ε_m of Popovics model which is available from normal strength to high strength concrete. Assuming that the observed Young's modulus is approximately equal to one obtained by Popovics model of Eq.2.3 at one third of the maximum strength, the next Eq. 2.7 is derived.

$$\frac{1}{3} = \sigma_B \frac{n \left(\frac{\sigma_B}{3E_C} \cdot \varepsilon_m \right)}{n - 1 + \left(\frac{\sigma_B}{3E_C} \cdot \varepsilon_m \right)^n} \quad (2.7)$$

Replacing $X = \frac{\sigma_B}{3E_C} \cdot \varepsilon_m$ into Eq. 2.7, the next Eq. 2.8 is derived.

$$f(X) = X^n - 3nX + n - 1 = 0 \quad (2.8)$$

$$\text{when } n=1, X=0 \quad (2.9)$$

$$\lim_{n \rightarrow \infty} X = \frac{1}{3} \quad (2.10)$$

Where, it is difficult to obtain the solution of positive X , X is approximately defined as Eq. 2.11.

$$X = \frac{1 - 1/n}{3} \quad (2.11)$$

Using Eq. 2.11, strain at the maximum stress is expressed as Eq. 2.12.

$$\varepsilon_m = \frac{\sigma_B}{E_C \left(1 - 1/n \right)} \quad (2.12)$$

From Eq. 2.12, experimental constant n is expressed as Eq. 2.13.

$$n = \frac{1}{1 - \frac{\sigma_B}{E_C} \cdot \varepsilon_m} \quad (2.13)$$

Experimental constant n depends on σ_B , E_C and ε_m . Assigning observed values of σ_B , E_C and ε_m to Eq. 2.13, the

relation between σ_B , and n is shown in Fig. 2.5. It is usually considered that the high strength concrete is more brittle than low strength concrete. Because experimental constant n was not proportional to compressive strength, Murakami proposed as Eq. 2.14. The model of relationship between stress and strain curves of the concrete should be expressed from low strength to high strength. Eq. 2.15 was obtained from the results of material test with least-squares method. Because coefficient of 0.0212 is in the same range as Murakami model, Murakami model was applied for the test results in this study.

$$\text{Modified by Murakami} \quad n = \exp(0.0256\sigma_B) \quad (2.14)$$

$$\text{Regression formula} \quad n = \exp(0.0212\sigma_B) \quad (2.15)$$

Comparisons between the values calculated by the above equations and observed results of strain at the maximum stress are shown in Fig. 2.6. The calculated value could express that the strain at the maximum stress becomes large when compressive strength decreased. The comparisons between the value calculated and observed stress strain curves were shown in Fig. 2.7. The modified Popovics model could predict the observed stress strain curves from the initial stage to the final.

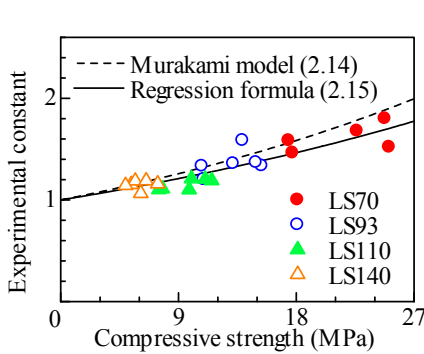


Fig. 2.5 Experimental constant vs. compressive strength

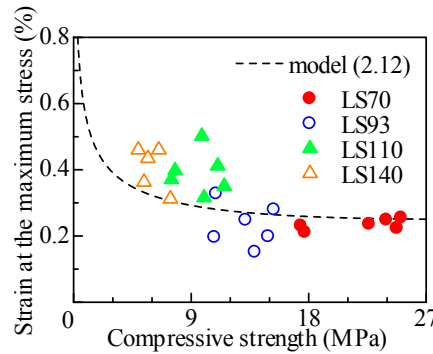


Fig. 2.6 Strain at the maximum stress vs. compressive strength

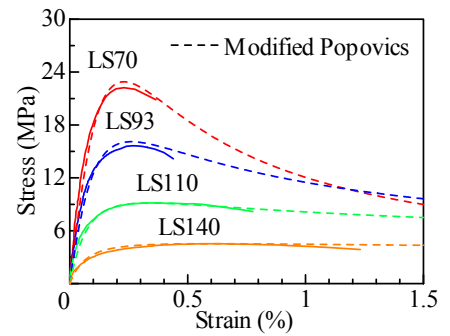


Fig. 2.7 Comparisons between modified Popovics model and observed stress strain curves

3. EXPERIMENTS OF RC BEAMS

3.1. Experimental Overview

3.1.1. Specimen

A total number of specimens was three. Common factors in the specimens were section (200x280mm), clear span (840mm), and shear span ratio (1.5). Arrangement of longitudinal reinforcing bars was 4-D13 (yield stress $\sigma_y=390\text{MPa}$). Considered parameters were concrete compressive strength (9 or 18MPa) and amount of stirrup (0.14 or 0.35%). Prepared beam specimens are summarized in Table 3.1. The configuration and bar arrangements are shown in Fig. 3.1.

3.1.2. Concrete

The summaries of mix properties for concrete are shown in Table 3.2. Mechanical properties of concrete are shown in Table 3.3. The advanced AE water reducing agent was used at mixing for casting concrete.

3.1.3. Reinforcement bar

D13 (SD390) was used for longitudinal reinforcing bar, and D6 (SD295A) was used for stirrup. The mechanical properties are shown in Table 3.4.

3.1.4. Force application and measuring method

The monotonic loadings under the anti-symmetric moment were subjected to the beam specimens. The electric

instruments to measure displacement in every place and the strain gages to measure strain of the reinforcing bars were mounted on the specimens.

Table 3.1 Summaries of beam specimens

Specimen	Section $b \times D$ (mm)	Concrete strength (MPa)	Longitudinal reinforcement	Stirrup reinforcement
18-14	200 × 280	18	4-D13 (SD390) $p_t = 1.01(\%)$	2-D6@200 (SD295) $p_w = 0.14$
09-14		9		
09-35				

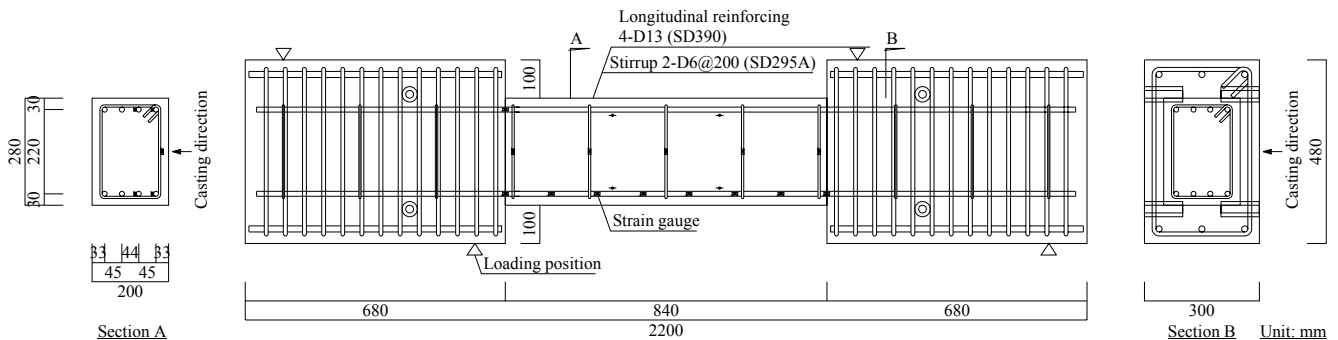


Fig. 3.1 Configuration and bar arrangements (stirrup ratio 0.14%)

Table 3.2 Summaries of mix properties for concrete

Mix type	Water cement ratio (%)	Cement (kg/m ³)	Water (kg/m ³)	Sand (kg/m ³)	Aggregate (kg/m ³)	Advanced AE water reducing agent (kg/m ³)	Slump (mm)	Sand Percentage (%)
Fc9	110	195	215	959	827	1.17	180	55
Fc18	80	269	215	892	835	1.61	180	53

Table 3.3 Mechanical properties of concrete

I.D.	σ_B (MPa)	E_C (GPa)	ε_m (%)	σ_{sp} (MPa)
Fc9	10.7	1.89	0.18	1.25
Fc18	18.3	2.41	0.11	2.02

σ_{sp} : concrete splitting strength

Table 3.4 Mechanical properties of steel

type	σ_y (MPa)	E_S (GPa)	ε_y (%)	σ_t (MPa)
D13(SD390)	403.3	19.5	0.21	593.0
D6(SD295A)	328.0	16.1	0.43	497.7

σ_t : tensile strength, σ_y : yield strength

E_S : Young's modulus of re-bar, ε_y : yield stress

3.2. Experimental Results of the Beam Test

3.2.1. Final Crack patterns

Crack patterns at the final stage of the specimens are shown in Fig. 3.2. For specimen (18-14), shear cracks and flexural cracks consecutively occurred at drift of 1/400rad.. Maximum strength was recorded at drift of 1/200rad.. Width of shear cracks increased rapidly at drift of 1/100rad. and strength decreased simultaneously. When fracture of the stirrup occurred at drift of 1/33rad., the specimen finally reached to shear failure mode. For specimen (09-14), shear cracks and flexural cracks occurred at drift of 1/400rad.. After reaching to drift of 1/200rad., bond splitting cracks occurred along the positions of the longitudinal reinforcing bars, shear cracks and bond splitting cracks progressed. This specimen showed the dual failure mode of the shear and bond failure at the final stage. For specimen (09-35), shear cracks and flexural cracks occurred as same as other two specimens. This specimen finally showed bond splitting failure mode.

3.2.2. Relationship between shear force and drift

Fig. 3.3 shows relationship between shear force and drift. The maximum strength, the ultimate displacement at

80% of the maximum strength, the occurrence of the flexural crack and the shear crack are point out in the figure. Strength of specimen (18-14) decreased rapidly to 80% of the maximum strength when drift exceeded 1/100rad.. Strength of specimen (09-14), decreased gradually after the maximum strength. Shear deflection curves of specimen (09-35) and specimen (09-14) were approximately same except for the maximum strength. Shear deflection curve of both specimens was more ductile than that of specimen (18-14) because amount of stirrup in both specimens were relatively large.

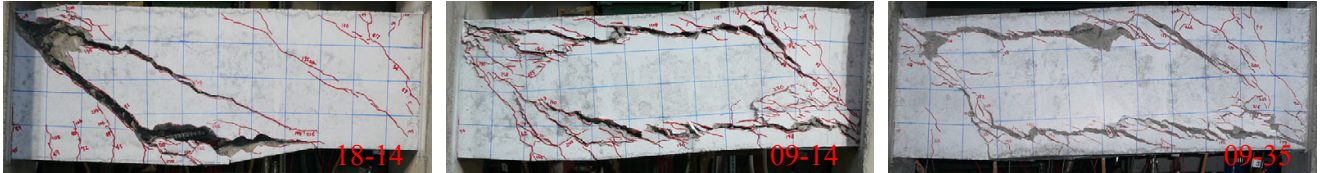


Fig. 3.2 Crack patterns at the final stages

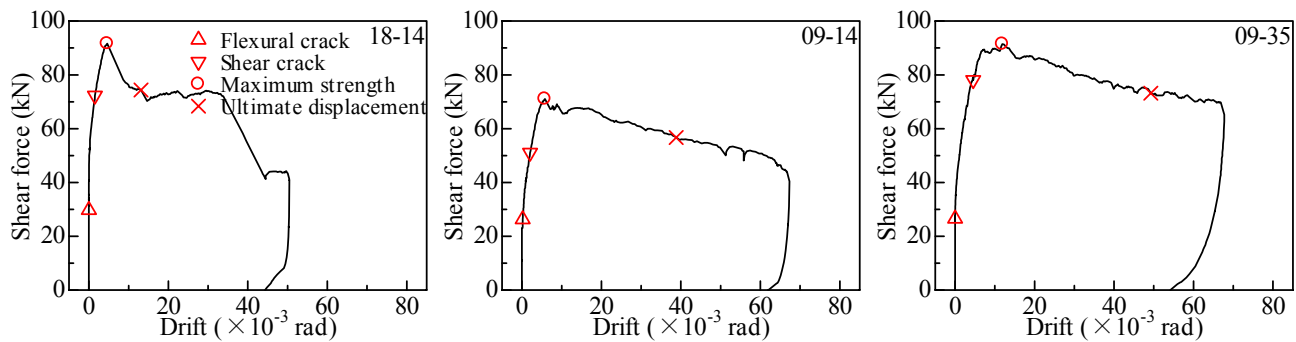


Fig. 3.3 Shear force-drift relation

4. THE COMPATIBILITY OF THE CURRENT EVALUATION TYPE

4.1. Maximum Load

Table 4.1 shows summary of the observed maximum strength and shear and bond capacity calculated by each formula. Shear capacity was calculated by Design Guideline for Earthquake Resistant Reinforced Concrete Buildings Based on Ultimate Strength Concept^[7] (A method of AIJ “ UQ_s ”), and by Standard for Structural Calculation of Reinforced Concrete Structures -Based on Allowable Stress Concept^[6] (Arakawa “ AQ_s ”). Bond capacities were calculated by theoretical formula proposed by Maeda-Otani^[8] (“ MQ_b ”), and Fujii-Morita^[9] (“ FQ_b ”). For calculated shear capacity, the maximum strength of specimen (18-14) which showed shear failure mode approximately agrees with the value calculated by A method. The values calculated by “Arakawa” have trend to overestimate the observed values. The maximum strength of specimen (09-35) which showed bond failure mode agrees with the value calculated by Maeda-Otani’s equation. For specimen (09-14) which showed the dual failure mode of the shear and bond failure, the maximum strength agrees with both the value calculated by A method and by Maeda-Otani’s formula.

Table 4.1 Summary of observed and calculated strength

Specimen	Observed maximum strength EQ_u (kN)	Shear capacity (kN)				Bond capacity (kN)			
		A method of AIJ UQ_s		Arakawa AQ_s		Maeda-Otani MQ_b		Fujii-Morita FQ_b	
		Calculated value (kN)	EQ_u/UQ_s	Calculated value (kN)	EQ_u/AQ_s	Calculated value (kN)	EQ_u/MQ_b	Calculated value (kN)	EQ_u/FQ_b
18-14	91.6	87.5	1.05	97.5	0.94	99.4	0.92	84.6	1.08
09-14	71.0	71.3	1.00	82.5	0.86	73.9	0.96	61.2	1.16
09-35	91.5	122.2	0.75	98.1	0.93	84.6	1.08	64.9	1.41

5. CONCLUSIONS

In this research, in order to provide the method for seismic evaluation of the existing low strength concrete buildings, the experimental tests using low strength concrete were performed. First, method to manufacture low strength concrete was proposed. Second, the monotonic loading tests under the anti-symmetric moment with one-third scaled RC beams were carried out to obtain the shear and bond characteristics of RC members used low strength concrete. The following concluding remarks were obtained from the test results and discussions.

- 1) It is able to manufacture low strength concrete of 9MPa with the mixture of water cement ratio 110%
- 2) In Young's modulus and compressive strength relation, formula of New RC (Eq. 2.2) is applicable for low strength concrete.
- 3) When compressive strength becomes low, strain at the maximum stress increase.
- 4) Stress strain curves of low strength concrete can be expressed by modified Popovics model.
- 5) Shear strength calculated by a method of AIJ agrees with observed maximum strength of the shear failure well.
- 6) Formula of Arakawa used for seismic evaluation have trend to overestimate observed shear strength.
- 7) Bond capacity calculated by Maeda-Otani formula agrees with observed maximum strength of the bond failure well.

REFERENCE

- [1] SAKAMAKI, K. HIROSAWA, M. SHIMIZU, Y. ZHOU, J. (2001). Research on Concrete Strength of Existing Reinforced Concrete Buildings (Part1, Part2). *Summaries of technical papers of Annual Meeting Architectural Institute of Japan*. **C-2:Structures IV**, 801-804.
- [2] TAKANO, F. OSHIMA, S. TERAMOTO, T. (2002). Seismic Assessment of Existing RC School Buildings in Tokyo (Part1). *Summaries of technical papers of Annual Meeting Architectural Institute of Japan*. **C-2:Structures IV**, 867-868.
- [3] The Japan Building Disaster Prevention Association. (2001). The Standard for Seismic Evaluation of Existing Reinforced Concrete Building, The Japan Building Disaster Prevention Association, Japan.
- [4] Architectural Institute of Japan. (1999) Recommendation for Practice of Mix Design of Concrete, Architectural Institute of Japan, Japan.
- [5] Architectural Institute of Japan. (1997) Japanese Architectural Standard Specification for Reinforced Concrete Work JASS5, Architectural Institute of Japan, Japan.
- [6] Architectural Institute of Japan. (1999) Standard for Structural Calculation of Reinforced Concrete Structures -Based on Allowable Stress Concept-, Architectural Institute of Japan, Japan.
- [7] Architectural Institute of Japan. (1990) Design Guideline for Earthquake Resistant Reinforced Concrete Buildings Based on Ultimate Strength Concept, Architectural Institute of Japan, Japan.
- [8] OTANI, S. MAEDA, M. (1994). An Equation for Bond Splitting Strength Based on Action between Deformed Bars and Concrete (Part1). *Summaries of technical papers of Annual Meeting Architectural Institute of Japan*. **C-2:Structures II**, 655-656.
- [9] FUJII, S. MORITA, S. (1982). SPLITTING BOND CAPACITIES OF DEFORMED BARS Part1 Experimental studies on main factors influencing splitting bond failure. *Transactions of the Architectural Institute of Japan*. **No.319**, 47-55.